ARTICLE

Check for updates

Translational Therapeutics

Tumour immune microenvironment in resected thymic carcinomas as a predictor of clinical outcome

Giovanni Bocchialini[1,2], Ana-Iris Schiefer[3], Leonhard Müllauer[3], Jürgen Thanner[1], Jonas Bauer[1], Felizia Thaler[1], Maria Laggner[1], Cecilia Veraar[4], Walter Klepetko[1], Konrad Hötzenecker[1], José Ramon Matilla[1], Hendrik Jan Ankersmit[1,5] and Bernhard Moser[1]✉

BACKGROUND: The spatial distribution of tumour-infiltrating lymphocytes (TILs) is a novel descriptor characterising the tumour immune microenvironment (TIME). The aim of our study was to assess whether a specific TIME of surgically resected thymic carcinoma (TC) can predict tumour invasiveness, recurrence or survival.
METHODS: Digital microscopy was performed on 39 TCs immunohistochemically stained to investigate the activation of the immune checkpoint pathway (PD-L1/PD-1), along with density and spatial distribution of TILs phenotypes (CD3+, CD4+, CD8+, FOXP3+, CD56+). The impact of PD-L1 and TIL density considering the intratumoural (*i*TILs) and stromal (*s*TILs) distribution on pathological characteristics and clinical outcomes were analysed.
RESULTS: In early TC stages, we observed a higher total density of CD3+ ($p = 0.05$) and CD8+ ($p = 0.02$) TILs. PD-L1 was expressed in 71.8% of TCs. In advanced TC stages, we observed a lower density of CD3+ ($p = 0.04$) and CD8+ ($p = 0.01$) *i*TILs compared to early stages. Serum concentrations of PD-L1 were significantly higher in TCs compared to healthy controls: 134.43 ± 18.51 vs. 82.01 ± 6.34 pg/ml ($p = 0.001$), respectively. High densities of stromal CD4+ TILs (54 vs. 32%, $p = 0.043$) and CD8+ TILs (65 vs. 17%, $p = 0.048$) were associated with improved freedom from recurrence (FFR) and cause-specific survival (CSS). High density of FoxP3+ TILs were associated with improved FFR ($p = 0.03$) and CSS ($p = 0.003$).
DISCUSSION: Mapping TIL subpopulations complement the armamentarium for prognostication of TC outcomes. The improved outcome in patients with high density of TILs supports the use of immune checkpoint inhibitors in TC patients.

British Journal of Cancer (2022) 127:1162–1171; https://doi.org/10.1038/s41416-022-01875-7

INTRODUCTION

Thymic epithelial tumours (TETs) are rare neoplasms with an annual incidence of 3/1,000,000, with no consistent gender predilection [1]. TETs are classified according to the World Health Organisation (WHO) histopathological classification into thymomas (WHO types A, AB, B1, B2 and B3) and thymic carcinomas (TCs; WHO type C) based on the morphology of epithelial tumour cells and proportion of the non-tumoural lymphocytic component [2]. Staging according to the Masaoka–Koga classification [3] and the tumour–node–metastasis (TNM)-based staging system for thymic malignancies [4] are currently the main reference tools driving the therapeutic strategies [5].

Improving the prognostic stratification of patients affected by TC with biological and anatomical tumour features may optimise the selection of patients for neoadjuvant and adjuvant treatments. Surgical complete resection is the most effective therapeutic modality for treating TETs and induction therapies are employed for cases that are deemed non-resectable on initial clinical staging [6, 7]. Common neoadjuvant chemotherapeutic treatments for TC patients are cisplatin–doxorubicin–cyclophosphamide or carboplatin–paclitaxel regimens with overall response rates >50% [8–10]. Novel radiotherapeutic techniques such as intensity-modulated radiation therapy and proton beam therapy may change the landscape of multidisciplinary TC treatment substantially reducing radiation exposure to adjacent organs at risk resulting in reduced long-term toxicities [11].

Immune checkpoint inhibitors (ICIs) are a novel therapeutic option in cancer treatment. The immune checkpoint pathway programmed cell death 1 (PD-1)/programmed cell death ligand 1 (PD-L1) plays a pivotal role in immune system regulation and homoeostasis. Malignant tumour cells harbour the potential to exploit those same pathways to induce immune suppression and escape anti-tumour immunity [12]. PD-L1 (B7-H1, CD274) is an immunomodulatory glycoprotein belonging to the B7-family. It is expressed by antigen-presenting cells as a negative regulator of the immune response in healthy human tissue where it mediates immune tolerance. PD-1 is a co-inhibitory receptor belonging to the CD28 family. It is expressed on T cells, B cells, natural killer (NK) cells, myeloid cells and activated monocytes. PD-1 binds PD-L1 to inhibit phosphatidylinositol 3-kinase/Akt, which reduces T cell

[1]Department of Thoracic Surgery, Medical University of Vienna, Vienna, Austria. [2]Thoracic Surgery, Department of Medicine and Surgery, University Hospital of Parma, Parma, Italy. [3]Department of Pathology, Medical University of Vienna, Vienna, Austria. [4]Department of Anaesthesiology, General Intensive Care and Pain Medicine, Medical University of Vienna, Vienna, Austria. [5]Head FFG Project "APOSEC", FOLAB Surgery, Medical University of Vienna, Vienna, Austria. ✉email: bernhard.moser@meduniwien.ac.at

Received: 28 July 2021 Revised: 5 May 2022 Accepted: 31 May 2022
Published online: 24 June 2022

activity and suppresses T cell-mediated interleukin (IL)-2 production. Furthermore, PD-L1 is upregulated in various malignancies and facilitates tumour growth and progression by inhibiting T cell response, allowing tumours to evade host-immune surveillance mechanisms [13]. The PD-1/PD-L1 pathway has been identified as a target for cancer immunotherapy with clinical success across a variety of tumour types [14] and recently also in surgical settings as neoadjuvant treatment [15].

The tumour immune microenvironment (TIME) [16] differs across cancer types [17] as well as between patients with the same disease [18]. Various populations of T-lymphocytes, B-lymphocytes, dendritic, NK, regulatory T (Tregs) cells and myeloid-derived suppressor cells, macrophages and neutrophils contribute to TIME composition. Type, density and location of tumour-infiltrating lymphocytes (TILs) involved in the adaptive and innate arms of the immune system constitute the predominant immune cell population of TIME, defining the host immune response to the tumour, which has prognostic significance in many solid malignancies [19–22]. Deeper analysis of complexity within the TIME and the tumour–host microenvironmental interplay could help to find novel prognostic and predictive biomarkers to identify patients who could benefit from ICI as induction treatment and optimise long-term management deploying adjuvant immunotherapies. While it is difficult to assess the chronological events shaping individual TIME in clinical practice, the histological specimen at the time point of curative resection provides an overview of the immune response against the tumour. Previous studies investigating PD-L1 in TETs have shown high expression in TCs; however, the impact on outcome remained unclear [23–25].

Recent research revealed that the spatial arrangement of TILs subpopulations in patients with lung cancer affects survival [26]. The spatial architecture of TILs in TETs as well as their prognostic role have not been determined. Also, there is no established methodology for TIL quantification in TETs. The aim of our study was to assess whether a specific TIME of surgically resected TCs might predict tumour invasiveness and progression, as well as recurrence and survival. To this end, we investigated the activation of the immune checkpoint pathway (PD-L1 and PD-1) in TCs, along with density and spatial distribution of TILs phenotypes (CD3+, CD4+, CD8+, FOXP3+, CD56+).

MATERIALS AND METHODS

Patient cohort and tissue sampling

Tumour tissue specimens were collected from 53 patients affected by TC who underwent surgical resection from 2000 to 2020 at the Thoracic Surgery Unit of University Hospital of Vienna, Austria. This retrospective study was approved by the Institutional Ethics Committee of the Medical University of Vienna (EC#1053/2016) and conformed to the ethical guidelines of the Declaration of Helsinki. Written informed consent was provided by all patients. All pathologic diagnoses were confirmed by experts in thymic pathology (LM and A-IS) based on the fourth edition of the WHO classification of thymic tumours [2]. TCs were classified according to the Masaoka–Koga [4] and Eighth TNM [5] staging systems. Out of 53 patients, 14 were excluded from the study due to the poor tissue quality. Thus, 39 patients with adequate histological tissue and complete clinicopathological data retrieved from available electronic medical records were eligible for this study. One patient who died from post-operative complications was excluded from the outcome analysis. The patient data follow-up was last updated in January 2021.

Immunohistochemical staining and digital image analysis

Serial tissue sections (2 µm thickness) were cut from formalin-fixed and paraffin-embedded specimens, processed with automated Leica Bond-III Immunostainer (Leica Camera, Wetzlar, Germany) and stained for all seven markers (Fig. 1). See Supplementary Material 1 for the list of primary antibodies and their detection. Stained slides were digitalised at high-volume scanning using an inverted Microscope Nikon Ti-Eclipse (Nikon, Tokyo, Japan) connected to Nikon NIS-AR Elements Software for acquisition and processing. Positively stained cells were automatically counted using the open-source software QuPath v0.2.3 [27–30]. This digital microscopy system provides high-fidelity reproducibility of TIL counting and eliminates interobserver variability. Digital analyses were performed previously selecting region of interest (ROI) from a unique scanned slide. The image analysis workflow consisted of several steps. First, the manual annotation of the two ROIs on each histological slide. The ROIs were: intratumoural area (IT) and stromal area (S), as described afterwards. Second, the whole area was analysed. Cell detection parameters for each marker were optimised by applying the cell detection across all cases and are listed in Supplementary Material 2 for reproducibility. TC diagnosis was established by experts in thymic pathology. Two expert pathologists (LM and A-IS) oversaw processing of all pathological specimens and immunohistochemical techniques. Specificity of staining was checked by pathologists in every case. Technical set-up for image processing and image analysis as well as the analysis was performed by GB, JB, LM and A-IS. The ROIs were selected including an area representative of the whole specimen and selected regions were validated by a pathologist (A-IS). Compared to other studies, large areas were analysed (range 6–22 mm^2), to overcome the variability of different areas. The parameters for positive cell detection were set manually for each marker and were the same for all samples. To ensure the reproducibility of our data obtained through digital analysis, specimens were randomly selected and manually checked for plausibility. All image processing, analysis and scoring was blinded to outcomes.

PD-L1 and TIL analysis

The density (number of cells/mm^2) of each TIL phenotype was computed on the total area (*total*-TILs, TILs) and according to their spatial distribution in relation to neoplastic cells using ROI at digital microscopy. TILs were categorised into intratumoural (*i*TILs) and stromal (*s*TILs) according to the guidelines from the International Immuno-Oncology Biomarkers Working Group [31]: *i*TILs are located within the neoplastic tissue and have either cell-to-cell contact with tumour cells or localised within 20 µm linear distance from cancer cells; *s*TILs are defined when dispersed within tumour stroma without direct contact with carcinoma or exhibit >20 µm linear distance from cancer cells. This linear distance of tolerance was chosen in accordance with previous study [26], with the rationale that within 20 µm cell-to-cell bio-humoral crosstalk seems feasible. All measurements were obtained by virtual microscopic examination set at ×200 magnification. Median values of each quantitative TIL parameters were used as cut-off to distinguish *high* vs. *low* subgroups. In addition, slides were semi-quantitatively scored and immunoreactivity for CD3, CD4 and CD8 was expressed as a score 0–3 (0: absent; 1: 1–33%; 2: 34–66%; 3: ≥67%) considering each marker as a percentage compared with the total amount of nucleated cells in the intratumoural and stromal compartments.

PD-L1 expression was scored using the Tumour Proportional Score (TPS), evaluated as the percentage of PD-L1-positive tumour cells with a complete or partial membranous staining at any intensity over the total tumour cells in the sample (range 0–100%). PD-L1 expression was categorised as: negative (expression <1%), positive (expression 1–50%), and highly positive (expression >50%) [32]. In addition, the semi-quantitative *H*-score was calculated, the proportion of cells with membranous PD-L1 expression (from 0 to 100%) was multiplied for the intensity of expression (from 1 to 3) with a score range of 0–300.

Enzyme-linked immunosorbent assay (ELISA) test measuring soluble PD-L1, soluble PD-1 and Bcl-2 on TC patient' serum and healthy controls was performed (Supplementary Material 3).

Statistical analyses

All analyses were performed using IBM SPSS Statistics v-25.0 (IBM, Armonk, NY, USA). Given the non-normal distribution of data tested by Kolmogorov–Smirnov test, the Kruskal–Wallis one-way analysis of variance test was used to compare the different groups. The correlation between two variables was measured by the Spearman's rank correlation coefficient. The following outcome measures as defined by ITMIG [33] and the European Society of Thoracic Surgeons Thymic Working group were tested: freedom from recurrence (FFR) and cause-specific survival (CSS): FFR included patients after complete surgical resection (R0) and was calculated from the date of surgery to the date of recurrence (censored observations: dead without recurrence and unknown recurrence status); CSS included all patients and was considered as death from TC (censored observations: unrelated death and unknown cause of death). Cox regression was performed to define potential independent factors influencing FFR and CSS and the multivariable model was fitted with the inclusion of the covariates that resulted statistically significant in the

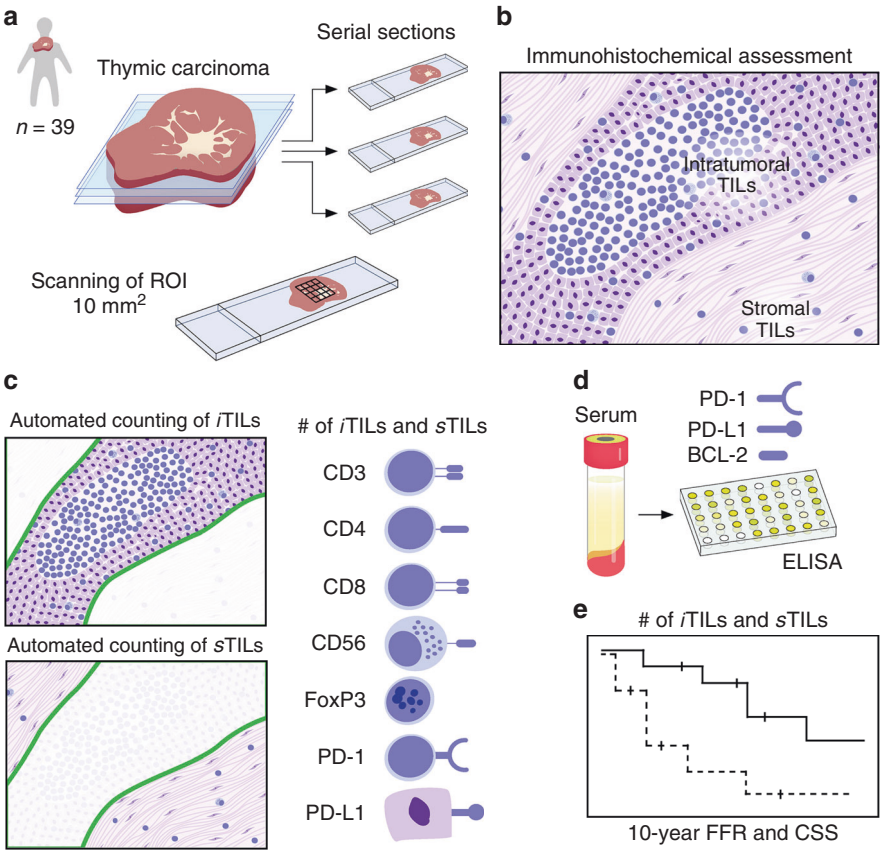

Fig. 1 Graphical overview of study design. Serial sectioning of TC specimens. Tumour tissues of 39 donors were included and an average area of 10 mm^2 of stained tissue sections was analysed (**a**). Scheme of TILs residing within the tumour or stroma (**b**). Tissue sections were stained for CD3, CD4, CD8, CD56, FoxP3, PD-1 and PD-L1. Numbers of *i*TILs and *s*TILs were automatically computed by high-volume scanning and digital microscopy (**c**). Serum levels of PD-1, PD-L1 and BCL2 were quantified in TC patients and healthy controls (**d**). Dichotomised numbers of TILs were analysed for recurrence and survival (**e**). CSS cause-specific survival, FFR freedom from recurrence, *i*TIL intratumoural tumour-infiltrating lymphocyte, *s*TIL stromal tumour-infiltrating lymphocyte, PD-1 programmed death 1 receptor, PD-L1 programmed death ligand 1, ROI region of interest, TIL tumour-infiltrating lymphocyte.

univariable model. Both FFR and CSS were censored at 10 years. Kaplan and Meier product limit method was employed to estimate survival and the log-rank was used to compare survival distributions of two samples and statistical significance was set at $p < 0.05$.

RESULTS

Clinicopathologic characteristics

The baseline clinicopathologic features of surgically resected TC patients studied by immunohistochemistry are detailed in Table 1.

Of the 39 TC cases, 19 patients (48.7%) received neoadjuvant therapies. Surgical complete resection was achieved in 32 cases (82.1%), with a microscopically confirmed negative surgical margin. The majority of TCs were squamous cell carcinoma histology ($n = 29$, 74.4%). Five TCs were combined thymomas: SCC combined with B2/B3 thymoma ($n = 2$) and SCC combined with B3 ($n = 2$). Median follow-up period for overall survival (OS) was 46 months (range 7–174); median FFR and CSS were 38 and 43 months, respectively.

Tumour immune microenvironment

TILs and PD-1. We detected CD3+, CD4+ and CD8+ TILs on all specimens of TC by immunohistochemistry (Fig. 2a). A subpopulation of TILs displayed FoxP3 or PD-1 expression. CD56+ cells were present in all TC specimens (Fig. 2b). The median densities for each TIL subpopulation in TCs were as follows: CD3+ 749.32 cells/mm^2, CD4+ 305.31 cells/mm^2, CD8+ 493.27 cells/mm^2, FOXP3+ 175.10 cells/mm^2, CD56+ 36.57 cells/mm^2, PD-1+ 15.40 cells/mm^2 (Supplementary Table 1). In early TNM stages, we observed a higher total density of CD3+ ($p = 0.05$) and CD8+ ($p = 0.02$) TILs compared to more advanced stages (Fig. 2c, d). This was in accordance with a higher infiltration of cytotoxic lymphocytes in early Masaoka–Koga stages ($p = 0.04$; Supplementary Fig. 1). An impact of neoadjuvant treatments on TIME constitution was observed, showing a trend of increased TIL density, although only CD56+ infiltration was statistically significant ($p = 0.024$; Supplementary Fig. 2).

Programmed cell death ligand 1. Membranous expression on tumour cells was computed using both TPS and *H*-score systems. PD-L1 staining was completely absent (TPS <1%) in 28.2% ($n = 11$) of cases, 43.6% ($n = 17$) of TCs expressed (TPS 1–49%) the ligand and high expression (TPS 50–100%) was present in 11 (28.2%) patients (Fig. 2e). No stromal expression of PD-L1 was found. Using PD-L1 *H*-score, there was a moderate strength of association between the density of CD3+ TILs ($r = 0.422$, $p < 0.0001$) (Supplementary Fig. 3). Considering the TPS score, high PD-L1 expression was associated with increased density of CD3+ ($p = 0.006$), CD4+ ($p = 0.01$), CD8+ ($p = 0.02$) and FOXP3+ ($p = 0.009$) TILs compared with the PD-L1-negative counterpart (Fig. 2f, g).

Spatial architecture of TILs

The TIL population was subdivided according to its spatial distribution into *i*TILs (Fig. 3a) and *s*TILs (Fig. 3d). The median densities of intratumoural vs. stromal TILs were: CD3+ 647.86 vs.

Table 1. Patient population.

	Number of patients: 39 (100%)
Clinical	
Gender	
Male	23 (59%)
Female	16 (41%)
Age (years), mean ± standard deviation	57.91 ± 16.02 (range 17–82)
Smoking status	
Never smoker	17 (43.6%)
Former/current smoker	22 (56.4%)
Pathological	
WHO histology	
Squamous cell TC	29 (74.4%)
Undifferentiated TC	8 (21.5%)
Lymphoepithelioma-like carcinoma	2 (5.1%)
Masaoka–Koga stage	
I	2 (5.1%)
II	10 (25.7%)
III	14 (35.9%)
IV	13 (33.3%)
pTNM stage (eighth ed.)	
I/II	13 (33.3%)
III/IV	26 (66.7%)
Myasthenia gravis	2 (5.1%)
Resection status	
R0	32 (82.1%)
R1/R2	7 (17.9%)
Treatment	
Induction treatments	
None	20 (51.3%)
Chemotherapy (ChT)	17 (43.5%)
Radiotherapy (RT)	2 (5.2%)
Adjuvant treatments	
None	13 (33.3)
Chemotherapy (ChT)	7 (18%)
Radiotherapy (RT)	19 (48.7%)
Survival (months) mean ± SD	
Freedom from recurrence	38.3 ± 49
Cause-specific survival	43.1 ± 46
Overall survival	46.5 ± 45

982.56 cells/mm^2, CD4+ 170.96 vs. 390.83 cells/mm^2 and CD8+ 465.70 vs. 436.85 cells/mm^2, respectively (Supplementary Table 1). In advanced TNM stages, we observed a shift from the intratumoural to the stromal compartment, particularly for CD3+ ($p = 0.04$) and CD8+ ($p = 0.01$) TILs compared to early stages (Fig. 3b–e). TCs expressing PD-L1 display higher intratumoural CD3+ ($p = 0.006$) and CD8+ ($p = 0.04$) TIL densities in comparison to TCs without membranous PD-L1 staining (Fig. 3c–f).

Survival analysis according to TILs density and spatial distribution

We examined the prognostic relationship of TILs density in TCs and their spatial distribution with recurrence and survival outcomes. In total, there were 20 recurrences and 17 TC-specific deaths. The overall number of CD3+ TILs did not significantly affect the clinical outcome (Supplementary Fig. 4).

Kaplan–Meier curves analysing the 10-year FFR are shown in Supplementary Fig. 5. Log-rank analysis showed an improved FFR with a high density of CD8+ TILs (65 vs. 17%, $p = 0.048$) and FOXP3+ TILs (49 vs. 29%, $p = 0.037$), as well as high CD4+ stromal TILs (54 vs. 32%, $p = 0.043$) infiltration.

The Kaplan–Meier curves analysing the 10-year CSS are shown in Fig. 4a–d, confirming the positive effect of lymphocytes located in the stroma. The CSS was in patients with *high* vs. *low CD8+* stromal *TILs* 76 vs. 39% ($p < 0.008$, Fig. 4d) and with *high* vs. *low CD4+* stromal *TILs* 91 vs. 32% ($p < 0.001$, Fig. 4b), respectively. High density of FOXP3+ TILs (84% vs. 33%, $p = 0.003$, Supplementary Fig. 5e) were associated with improved CSS.

No influence on recurrence and survival could be detected when CD56+ and PD-1+ TIL densities were dichotomised by their median values.

Univariable and multivariable analyses of FFR and CSS

Univariable and multivariable analyses for FFR and CSS were employed to test for potential prognostic factors: clinical characteristics, PD-L1 expression, and TILs infiltration as well as their spatial distribution (Supplementary Tables 2 and 3). Univariable analysis on clinical parameters revealed that T stage and lymphovascular invasion were associated with lower FFR and CSS. Univariable analysis on immunohistochemical parameters showed that high density of stromal-CD4+, CD8+ and FoxP3+ TILs were associated with improved FFR; higher density of stromal-CD3+, CD4+, stromal-CD4+, CD8+, stromal-CD8+ and FoxP3+ TILs were associated with improved CSS. Statistically significant parameters at univariable analysis did not confirm their prognostic value at multivariable analysis.

Classifying TC based on PD-L1 and T cell infiltration

To predict response to PD-1/PD-L1 blockade, a classification of tumours based on their PD-L1 status and prevalence (TILs+) or absence (TILs−) of TILs has been proposed [34]. TCs were considered as TILs+ when displaying a high density of sCD4+ and/or sCD8+ TILs (immunoreactivity score 2–3), which had prognostic value in our study. Four categories describing the TIME are: type I adaptive immune resistance (PD-L1+/TILs+: 20 patients, 51.3%), type II immunological ignorance (PD-L1−/TILs−: 6 patients,15.4%), type III intrinsic induction (PD-L1+/TILs−: 8 patients, 20.5%), and type IV tolerance (PD-L1−/TILs+: 5 patients, 12.8%), respectively.

In the survival analyses, type I and IV TIME, corresponding to TILs+ tumours, have shown a better CSS compared with the other groups (log rank analysis: I vs. II $p < 0.0001$, I vs. III $p < 0.006$; IV vs. II $p < 0.019$, IV vs. III $p < 0.027$) (Fig. 5).

Detection of PD-L1, PD-1 and BCL-2 in the serum

Serum concentrations of PD-L1 were significantly higher in TCs ($n = 12$) compared to healthy controls ($n = 45$): 82.01 ± 6.34 Controls vs.134.43 ± 18.51 pg/ml TCs ($p = 0.001$) (Supplementary Material 2). In contrast, serum concentration of PD-1 showed no statistically significant differences between controls ($n = 47$) and TCs ($n = 17$) 2780.98 ± 517.42 vs. 1574.59 ± 712.97 pg/ml respectively ($p = 0.125$). Furthermore, there was no difference in the antiapoptotic protein BCL-2 serum concentrations between controls ($n = 16$) and TCs ($n = 18$) 145.27 ± 109.39 vs. 109.61 ± 59.07 ng/ml, respectively ($p = 0.932$).

DISCUSSION

The modern management of cancer patients is based on a multidisciplinary team, where the oncologist is guided by detailed pathologic and molecular characterisations of surgical or biopsy

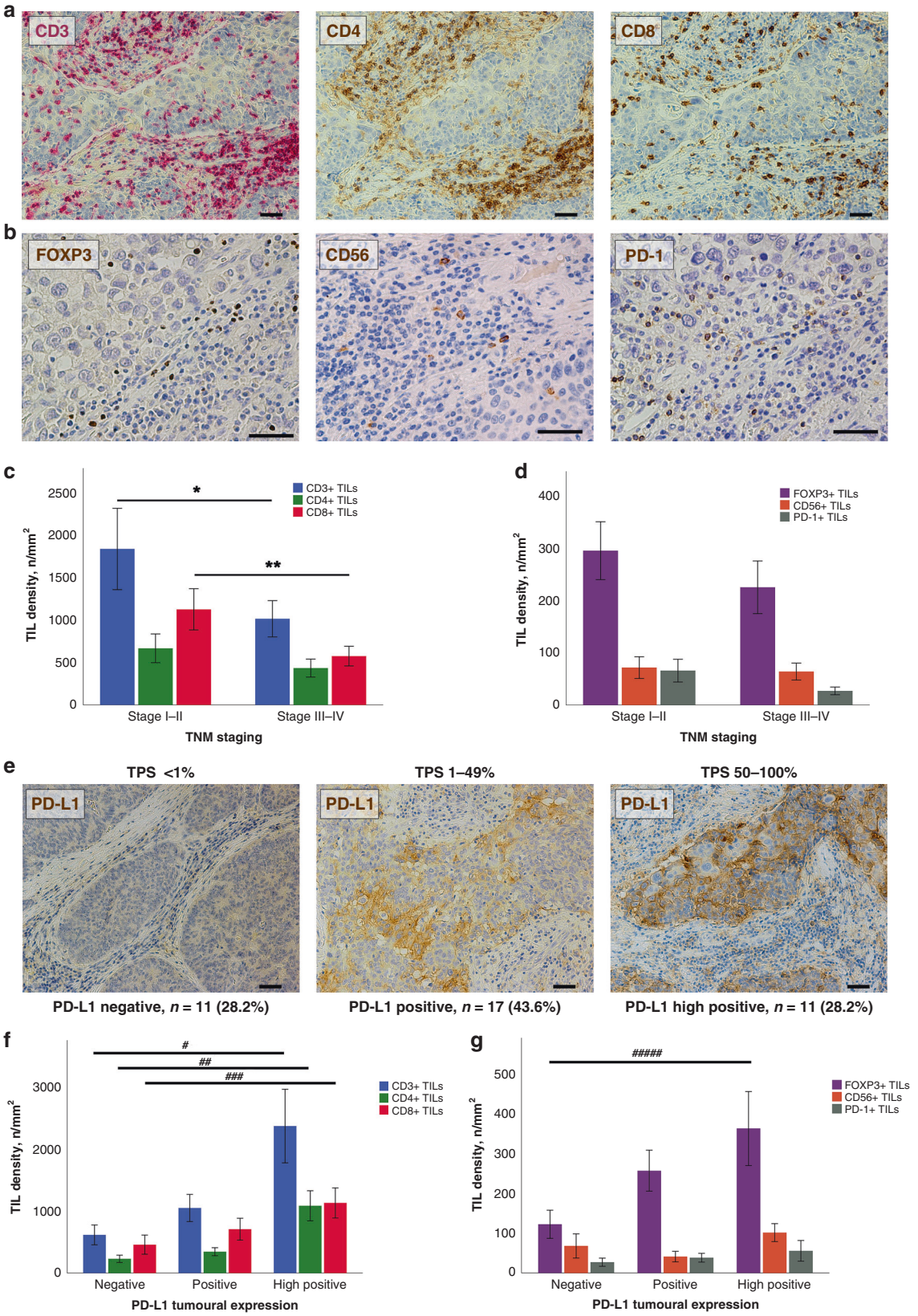

specimens, to identify patients who might benefit from follow-up or adjuvant treatments. With the advent of immunotherapy, the characterisation of patients' TIME has reached paramount biologic and clinical relevance.

The extreme inter- and intra-tumour variability in the magnitude of immune cell infiltrates obfuscates the real prognostic and predictive value of TIME, suggesting the need for careful assessment of TIL incidence and distribution. Correlating various

Fig. 2 Tumour-infiltrating lymphocytes and programmed death ligand 1 in thymic carcinoma. Immunohistochemistry on serial sections of a thymic SCC is displayed. Immunoperoxidase staining of CD3+ (red), CD4+ and CD8+ (brown) lymphocytes of a TC sample (**a**). Detection with brown peroxidase of FOXP3+, CD56+ and PD-1+ TILs in another area of the same case (**b**). Bar graphs showing a significantly decreased density of CD3+ and CD8+ TILs as well as decreased densities of CD4+, FOXP3+, CD56+ and PD-1+ TILs in advanced TNM stages ($^{*}p = 0.05$, $^{**}p = 0.02$) (**c**, **d**). Immunohistochemical detection of PD-L1 in TCs revealed different levels of expression. Representative micrographs are shown: no expression with TPS <1%, PD-L1 expression with TPS from 1 to 49% and high PD-L1 expression with TPS from 50 to 100% (**e**). Bar diagrams illustrating the increased density of TILs concomitant to high PD-L1 expression ($^{\#}p = 0.006$, $^{\#\#}p = 0.01$, $^{\#\#\#}p = 0.02$, $^{\#\#\#\#}p = 0.009$) (**f**, **g**). Scale bars: 100 µm (**a**, **e**) and 50 µm (**b**). TIL tumour infiltrating lymphocytes, PD-L1 programmed death ligand 1, TPS Tumour Proportional Score, TC thymic carcinoma, SCC squamous cell carcinoma, TNM tumour–node–metastasis staging system.

immune-cell densities with clinical aspects requires a large-scale tissue evaluation, which cannot be achieved on microscopic fields or on tissue microarrays. Virtual microscopy and digitally assisted analysis allow to evaluate large sections of tumours, thus providing a more suitable density estimation of the heterogeneous context of TIME. In our study, an extensive morphometric quantification of TIL subpopulations according to their location targeted with ROI was performed. The analysis on serial sections carries the advantage to acquire a more consistent view of the interplay between different immune phenotypes and their interaction with cancer cells.

Our findings regarding the relationship between TILs and tumour stage in TCs agree with other solid organ malignancies, such as non-small cell lung [35] or colorectal cancers [36]. We detected a higher density of total and intratumoural TILs, particularly CD3+ and CD8+ (analogous trends for the less frequent tumour-infiltrating cells) in early stages compared to advanced tumours, suggesting that specific immune cells favourably shape tumour environment countering disease progression and metastatic potential [20].

Although expression of PD-1 and PD-L1 as detected by immunohistochemistry has been associated with positive responses to ICI, its prognostic value in different tumour types is still undetermined and limited data for TETs have shown conflicting results [23, 24, 37]. A study on 69 TET cases employing tissue microarray found that high PD-L1 score was associated with higher WHO grade histology and stage, as well as worse clinical outcome [23]. Conflicting results were reported on 82 thymomas and 25 TCs: 54% of thymomas [37] were associated with high PD-L1 expression and with worse clinical outcome compared to no expression; conversely, high PD-L1 expression in TCs was associated with prolonged disease-free survival and OS, whereas increased PD-1+ TILs correlated with poor prognosis [24]. Our study confirmed the expression of PD-L1 in 71.8% of TCs with a trend towards better FFR (Supplementary Fig. 4) and reinforced by the observation of a direct correlation between high PD-L1 expression and increased TIL infiltration. This relationship suggests that PD-L1 expression by tumour cells might be upregulated as a result of a feedback mechanism against activation of host anti-tumour immunity. This hypothesis is supported by murine in vivo models of melanoma showing that expression of immunosuppressive molecules was induced following CD8+ TIL activation and interferon (IFN)-γ production [38].

Histological evaluation of TILs is emerging as a promising biomarker in solid tumours, reaching a level-IB evidence as a prognostic marker in triple-negative and Her-2 positive breast cancer [39]. In TCs, stage-dependent decline in immune cell infiltration critically contributes to tumour progression and may represent a valuable prognostic tool. In our TC cohort, the magnitude of TIL infiltration into the stromal compartment was a striking outcome predictor. Different FFR related to different TIME represents an additional instrument to define subsets of TC patients at high risk of relapse. The analysis of cytotoxic (CD8) and helper (CD4) T cells strictly in *stromal*-ROI has provided a better prognostic stratification regarding FFR and CSS instead of the *total*-ROI. In our view, TILs in stroma might control or reflect the immune responses against cancer cells, especially Th1 helper lymphocytes are critical in initiating and maintaining immune responses against cancer cells by secreting cytokines such as IL-2 and by activating antigen-presenting cells, including dendritic cells [21].

A correlation between regulatory (FoxP3+) T cells and favourable clinical outcome was observed in colorectal, head and neck, oesophageal cancers and haematologic malignancies. Conversely, lung, renal and hepatocellular carcinomas and melanoma Tregs were associated with unfavourable prognosis [40]. Thus, the prognostic value of FoxP3+ TILs in cancer remains controversial and its role is highly influenced by tumour site. To our knowledge, the role of FoxP3+ TILs in TCs has never been deeply explored. We observed a significantly lower rate of tumour recurrence and improved survival in TCs with *high*-FoxP3+ TIL density. The observation that in human cancers FoxP3+ Tregs suppress pro-tumourigenic effects by killing macrophages and monocytes supports our findings [41]. In addition, it has been demonstrated that adoptive immunotherapy with CD4+ CD45+ Tregs decreases tumour multiplicity through inducing apoptosis of intestinal tumours [42]. Thus, the thymus is a major site of Treg cell induction, where FoxP3 expression is initiated through a combination of antigen recognition and microenvironmental influences, justifying the prognostic role in this specific malignancy.

Specific immune contextures are considered as potential biomarkers to determine the disease stage, clinical outcome and therapeutic response [34]. Classification of TIME based on PD-L1 status and the presence or absence of TILs originally described by Teng distinguishes four categories: type I (PD-L1 positive with TILs: driving adaptive immune resistance), type II (PD-L1 negative without TILs: indicating immune ignorance), type III (PD-L1 positive without TILs: indicating intrinsic induction), and type IV (PD-L1 negative with TILs: indicating the role of other suppressors in promoting immune tolerance). The proportions of various human tumours that fit into each of these types, as defined by PD-L1/TILs status, likely depend on the tumour mutations and oncogenic drivers as well as the tissue they arise in. We documented in our TC cohort that >50% TCs were classified as type I tumours; with the second most frequent pattern being type III. It has been reported that patients with type I TIME are largely responding to ICI therapy and could benefit from single-agent therapy, as these tumours have evidence of pre-existing intratumour T cells that are turned off by PD-L1 engagement [43]. About 20% of TC patients displayed a type III TIME with constitutive PD-L1 expression on cancer cells powered by oncogenic signalling. For this group of patients, a therapeutic approach able to recruit lymphocytes into tumours is recommended: radiotherapy to promote immunogenic cell death to release neoantigens has been used to induce T cell responses in combination with PD-1 blockade [44]. TILs rich or "hot" TIME has shown a better CSS compared to TILs poor or "cold" TCs. In type IV, the absence of PD-L1 expression with an abundance of TILs has shown the best clinical outcome, supporting the anti-tumoural effect of CD4+ and CD8+ TILs where immune checkpoint pathway is shut down.

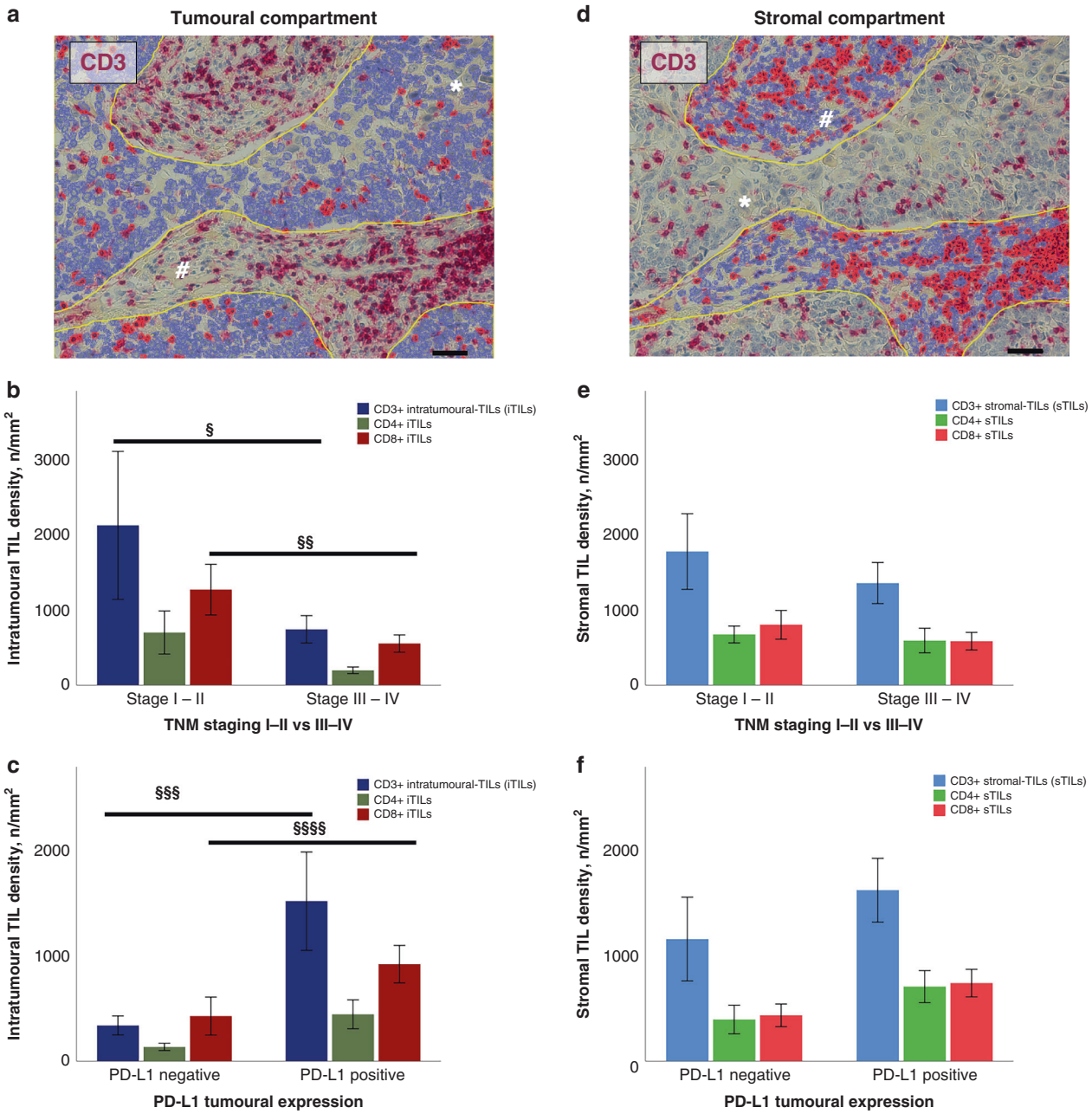

Fig. 3 Assessment of the spatial architecture of TILs using digital system. Region of interest (ROI) corresponding to tumour area and automated detection of CD3-positive infiltrating lymphocytes (red dots, iTILs) (**a**). Stromal area selected within the ROI and following automated detection of CD3-positive infiltrating lymphocytes (red dots, sTILs) (**d**). Bar graphs showing the different spatial distribution of TILs according to TNM stage ($^{§}p = 0.04$, $^{§§}p = 0.01$) (**b**–**e**) and PD-L1 expression ($^{§§§}p = 0.006$, $^{§§§§}p = 0.04$) (**c**–**f**). Asterisks (*) indicate tumour cells. Hashes (#) indicate stromal tissue. Scale bars: 100 µm. *i*TIL intratumoural-infiltrating lymphocyte, PD-L1 programmed death ligand 1, ROI region of interest, *s*TIL stromal-infiltrating lymphocyte.

Our study, besides supporting the relevance of the immune microenvironment, provides evidence that fine tuning of the local immune surveillance is critical for cancer evolution. At the time of surgery, a poorly infiltrated TIME cannot be considered an unchangeable condition but requires efforts to revert this detrimental event. To this end, decoding immune profiles, including the underlying chemokine network, might offer crucial information to optimise the use of immunotherapy in TCs. One of the promising approaches for rare cancers is the evaluation of clinical specimens, specifically tumour tissues. Thus, in the era of personalised therapy, the results of our investigation on the prognostic impact of the spatial architecture and density of TILs strongly support the notion that patient-specific TIME might improve the risk stratification of TCs, guiding adjuvant therapeutic strategies. Computer-aided diagnostics enable computational methods that extract spatio-morphologic predictive features, reducing inter-reader variability. From a mechanistic perspective of the association of PD-L1 and improved survival, PD-L1 expression may generally be a surrogate marker for an "inflamed" TIME, which is consistent with an effective host response to the tumour and improved survival as a result of native anti-tumour immunity. The association between PD-L1 expression and improved benefit from ICI in other tumour types raises the possibility that ICI may be an effective therapy for patients with TCs in association with surgery.

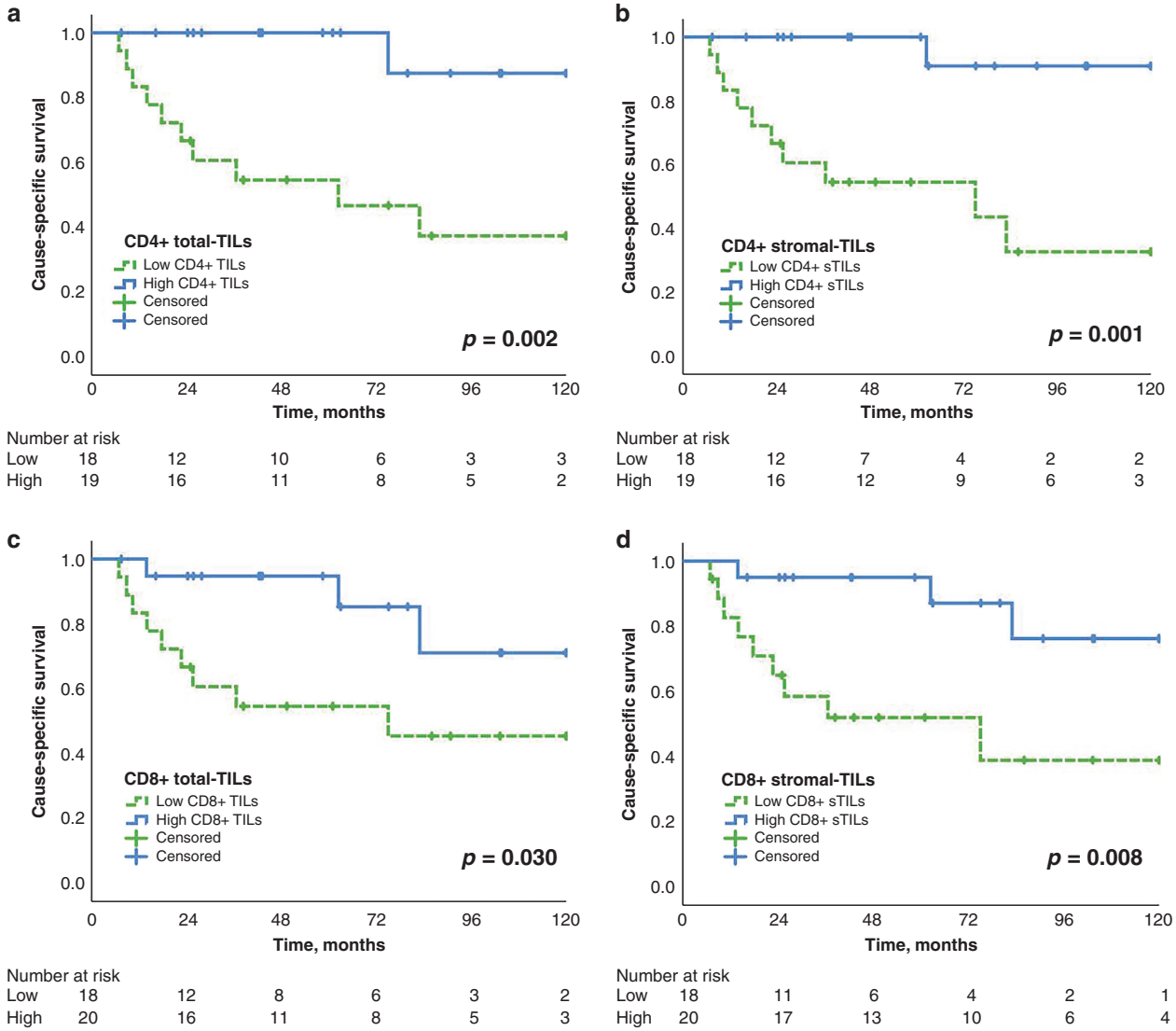

Fig. 4 Outcome analysis. Kaplan–Meier survival curves showing the impact of density and localisation of CD4+, CD8+ CSS (**a**–**d**) in thymic carcinoma patients. The median of respective TIL density was used to dichotomise into high and low groups. Log-rank test *p* values as well as the number of patients at risk are indicated. CSS cause-specific survival.

Ongoing clinical trials based on ICI have reported an acceptable clinical efficacy of anti-PD-1 antibodies for TETs [45, 46]. Considering that ICI could induce fatal adverse events [47], it is crucial to identify predictive tools to select patients who may benefit from ICI. The analysis of T cell profiles, cytokine production and T cell cytotoxicity of TILs in surgical specimens revealed that CD4 and CD8 single-positive T cells may play a crucial role for anti-tumour immunotherapy in B3/TC patients. A stronger in vitro T cell cytotoxicity and IFN-γ secretion in freshly isolated T cells from B3/TC tissue was observed when analysed in co-culture with tumour cells and anti-PD-1 antibody (nivolumab) compared to control (IgG4). In accordance with our findings, the authors reported that Tregs strongly infiltrate TETs with high TIL density [48]. Giaccone and Kim [49] recently reported long-term follow-up of 40 TC patients treated with anti-PD-1 antibody Pembrolizumab with a 22.5% response rate and a median duration of response of 3 years (median OS 2.1 years and 5-year OS of 18%). ICIs are generally well tolerated, but immune activation can occasionally cause severe toxicity. For this reason, identification of biomarkers foreseeing treatment responses and toxicity is an active area of research [50]. Many efforts are underway to identify circulating molecules suitable for clinical screening of TETs [51] or response to therapy. The value of soluble PD-1/PD-L1 remains unclear [52]. In our TC cohort, concentration of PD-L1 in serum were significantly higher in TCs compared to healthy controls. Conversely, the amount of soluble PD-1 and Bcl-2 between the two groups did not show any difference. No correlation between tissue expression and serum concentrations of PD-1 and PD-L1 was discovered. Further investigations on larger population are warranted to assess the role of PD-L1 as biomarker in TCs, an undertaking that will need multicentre efforts.

This study carries the characteristic weaknesses of research performed on orphan diseases [53]. Because of the necessity of analysing TC resection specimens, one limitation is that only patients who were candidates for surgical resection were available for this study. Patients not amenable to surgery because of nonresectability (organ infiltration deemed unresectable or metastasised patients) or patients with resectable disease but comorbidities not allowing surgery and/or anaesthesia were not accessible for this research effort. So, there is an obvious selection bias towards surgical patients. Patients who underwent chemotherapy and/or radiotherapy without surgical resection were not included. In order to increase the amount of available tumour tissue samples, this study was performed in a prospective and

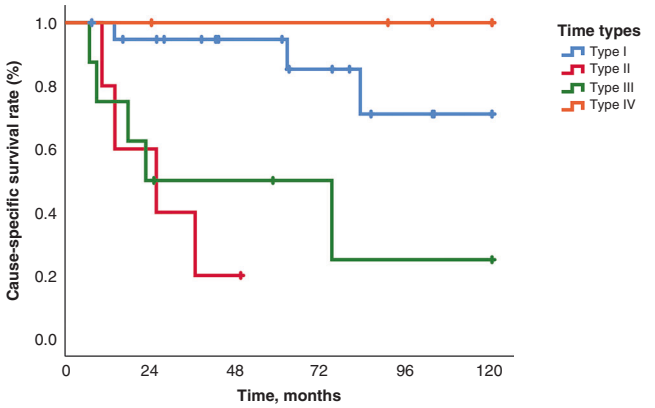

Type	I (PD-L1+, TILs+)	II (PD-L1−, TILs−)	III (PD-L1+, TILs−)	IV (PD-L1−, TILs+)
I ($n = 20$)	/	0.0001	0.006	0.252
II ($n = 6$)	**0.0001**	/	0.595	**0.019**
III ($n = 8$)	**0.006**	0.595	/	**0.027**
IV ($n = 5$)	0.252	0.019	0.027	/

Fig. 5 Survival analysis according to TIME types. Cause-specific survival according to the four tumour microenvironment types based on PD-L1 and TILs. Kaplan–Meier curves for each type: type I (PD-L1+/TILs+) adaptive immune resistance, type II (PD-L1−/TILs−) immunological ignorance, type III (PD-L1+/TILs−) intrinsic induction, and type IV (PD-L1−/TILs+) tolerance. At the bottom, the table shows the log-rank test between groups. PD-L1 programmed death ligand 1, TILs tumour infiltrating lymphocyte.

retrospective manner pooling patients after induction treatments. A larger series is needed to determine associations more robustly with outcomes in a more comprehensive multivariable analysis and validation of our findings. TC is a rare disease, thus only multicentre efforts will be able to accomplish the higher patient numbers for analysis.

In conclusion, TCs appear to carry a "hot" immune contexture displaying abundant PD-L1 expression and high TIL density. High stromal T helper and cytotoxic lymphocyte infiltration is related to better clinical outcome. A systematic analysis of TIME is warranted to develop biomarkers able to predict response to ICI treatments in patients with TC. Our findings support future study on the use of ICIs in neoadjuvant settings to increase complete resection rates as well as in adjuvant treatments to achieve systemic control of the disease following surgery.

DATA AVAILABILITY

All data generated or analysed during this study are included in this published article and its Supplementary Information files. The original data are with the first author available on demand.

REFERENCES

1. de Jong WK, Blaauwgeers JL, Schaapveld M, Timens W, Klinkenberg TJ, Groen HJ. Thymic epithelial tumours: a population-based study of the incidence, diagnostic procedures and therapy. Eur J Cancer. 2008;44:123–30. https://doi.org/10.1016/j.ejca.2007.11.004.
2. Marx A, Ströbel P, Badve SS, Chalabreysse L, Chan JK, Chen G, et al. ITMIG consensus statement on the use of the WHO histological classification of thymoma and thymic carcinoma: refined definitions, histological criteria, and reporting. J Thorac Oncol. 2014;9:596–611. https://doi.org/10.1097/JTO.0000000000000154.
3. Detterbeck FC, Nicholson AG, Kondo K, Van Schil P, Moran C. The Masaoka-Koga stage classification for thymic malignancies: clarification and definition of terms. J Thorac Oncol. 2011;6:S1710–6. https://doi.org/10.1097/JTO.0b013e31821e8cff.
4. Detterbeck FC, Stratton K, Giroux D, Asamura H, Crowley J, Falkson C, et al. The IASLC/ITMIG Thymic Epithelial Tumors Staging Project: proposal for an evidence-based stage classification system for the forthcoming (8th) edition of the TNM classification of malignant tumors. J Thorac Oncol. 2014;9:S65–72. https://doi.org/10.1097/JTO.0000000000000290.
5. Girard N, Ruffini E, Marx A, Faivre-Finn C, Peters S, on behalf of the ESMO Guidelines Committee. Thymic epithelial tumours: ESMO Clinical Practice Guidelines for diagnosis, treatment and follow-up. Ann Oncol. 2015;26:v40–55. https://doi.org/10.1093/annonc/mdv277.
6. Yano M, Sasaki H, Yokoyama T, Yukiue H, Kawano O, Suzuki S, et al. Thymic carcinoma: 30 cases at a single institution. J Thorac Oncol. 2008;3:265–9. https://doi.org/10.1097/JTO.0b013e3181653c71.
7. Ruffini E, Detterbeck F, Van Raemdonck D, Rocco G, Thomas P, Weder W, et al. Tumours of the thymus: a cohort study of prognostic factors from the European Society of Thoracic Surgeons database. Eur J Cardiothorac Surg. 2014;46:361–8. https://doi.org/10.1093/ejcts/ezt649.
8. Loehrer PJ Sr, Kim K, Aisner SC, Livingston R, Einhorn LH, Johnson D, et al. Cisplatin plus doxorubicin plus cyclophosphamide in metastatic or recurrent thymoma: final results of an intergroup trial. The Eastern Cooperative Oncology Group, Southwest Oncology Group, and Southeastern Cancer Study Group. J Clin Oncol. 1994;12:1164–8. https://doi.org/10.1200/JCO.1994.12.6.1164.
9. Kelly RJ, Petrini I, Rajan A, Wang Y, Giaccone G. Thymic malignancies: from clinical management to targeted therapies. J Clin Oncol. 2011;29:4820–7. https://doi.org/10.1200/JCO.2011.36.0487.
10. Berghmans T, Durieux V, Holbrechts S, Jungels C, Lafitte JJ, Meert AP, et al. Systemic treatments for thymoma and thymic carcinoma: a systematic review. Lung Cancer. 2018;126:25–31. https://doi.org/10.1016/j.lungcan.2018.10.018.
11. Willmann J, Rimner A. The expanding role of radiation therapy for thymic malignancies. J Thorac Dis. 2018;10:S2555–64. https://doi.org/10.21037/jtd.2018.01.154.
12. Pardoll DM. The blockade of immune checkpoints in cancer immunotherapy. Nat Rev Cancer. 2012;12:252–64. https://doi.org/10.1038/nrc3239.
13. Dong H, Strome SE, Salomao DR, Tamura H, Hirano F, Flies DB, et al. Tumor-associated B7-H1 promotes T-cell apoptosis: a potential mechanism of immune evasion. Nat Med. 2002;8:793–800. https://doi.org/10.1038/nm730. Erratum 2002;8:1039.
14. Topalian SL, Hodi FS, Brahmer JR, Gettinger SN, Smith DC, McDermott DF, et al. Safety, activity, and immune correlates of anti-PD-1 antibody in cancer. N Engl J Med. 2012;366:2443–54. https://doi.org/10.1056/NEJMoa1200690.
15. Forde PM, Chaft JE, Smith KN, Anagnostou SV, Cottrell TR, Hellmann MD, et al. Neoadjuvant PD-1 blockade in resectable lung cancer. N Engl J Med. 2018;378:1976–86. https://doi.org/10.1056/NEJMoa1716078. Erratum 2018;379:2185.
16. Binnewies M, Roberts EW, Kersten K, Chan V, Fearon DF, Merad M, et al. Understanding the tumor immune microenvironment (TIME) for effective therapy. Nat Med. 2018;24:541–50. https://doi.org/10.1038/s41591-018-0014-x.
17. Gentles AJ, Newman AM, Liu CL, Bratman SV, Feng W, Kim D, et al. The prognostic landscape of genes and infiltrating immune cells across human cancers. Nat Med. 2015;21:938–45. https://doi.org/10.1038/nm.3909.
18. Thorsson V, Gibbs DL, Brown SD, Wolf D, Bortone DS, Yang TH, et al. The Immune Landscape of Cancer. Immunity. 2018;48:812.e14–30.e14. https://doi.org/10.1016/j.immuni.2018.03.023. Erratum 2019;51:411–2.
19. Galon J, Costes A, Sanchez-Cabo F, Kirilovsky A, Mlecnik B, Lagorce-Pagès C, et al. Type, density, and location of immune cells within human colorectal tumors predict clinical outcome. Science. 2006;313:1960–4. https://doi.org/10.1126/science.1129139.
20. Fridman WH, Pagès F, Sautès-Fridman C, Galon J. The immune contexture in human tumours: impact on clinical outcome. Nat Rev Cancer. 2012;12:298–306. https://doi.org/10.1038/nrc3245.
21. Bremnes RM, Busund LT, Kilvær TL, Andersen S, Richardsen E, Paulsen EE, et al. The role of tumor-infiltrating lymphocytes in development, progression, and prognosis of non-small cell lung cancer. J Thorac Oncol. 2016;11:789–800. https://doi.org/10.1016/j.jtho.2016.01.015.
22. Mazzaschi G, Madeddu D, Falco A, Bocchialini G, Goldoni M, Sogni F, et al. Low PD-1 expression in cytotoxic $CD8^+$ tumor-infiltrating lymphocytes confers an immune-privileged tissue microenvironment in NSCLC with a prognostic and predictive value. Clin Cancer Res. 2018;24:407–19. https://doi.org/10.1158/1078-0432.CCR-17-2156.
23. Padda SK, Riess JW, Schwartz EJ, Lu Tian, Kohrt HE, Neal JW, et al. Diffuse high intensity PD-L1 staining in thymic epithelial tumors. J Thorac Oncol 2015;10:500–8. https://doi.org/10.1097/JTO.0000000000000429.
24. Yokoyama S, Miyoshi H, Nakashima K, Shimono J, Hashiguchi T, Mitsuoka M, et al. Prognostic value of programmed death ligand 1 and programmed death 1 expression in thymic carcinoma. Clin Cancer Res. 2016;22:4727–34. https://doi.org/10.1158/1078-0432.CCR-16-0434.
25. Tiseo M, Damato A, Longo L, Barbieri F, Bertolini F, Stefani A, et al. Analysis of a panel of druggable gene mutations and of ALK and PD-L1 expression in a series of thymic epithelial tumors (TETs). Lung Cancer. 2017;104:24–30. https://doi.org/10.1016/j.lungcan.2016.12.005.
26. Bocchialini G, Lagrasta C, Madeddu D, Mazzaschi G, Marturano D, Sogni F, et al. Spatial architecture of tumour-infiltrating lymphocytes as a prognostic parameter in resected non-small-cell lung cancer. Eur J Cardiothorac Surg. 2020;58:619–28. https://doi.org/10.1093/ejcts/ezaa098.

27. Bankhead P, Loughrey MB, Fernández JA, Dombrowski Y, McArt DG, Dunne PD, et al. QuPath: open source software for digital pathology image analysis. Sci Rep. 2017;7:16878. https://doi.org/10.1038/s41598-017-17204-5.
28. Jhun I, Shepherd D, Hung YP, Madrigal E, Le LP, Mino-Kenudson M. Digital image analysis for estimating stromal CD8+ tumor-infiltrating lymphocytes in lung adenocarcinoma. J Pathol Inform. 2021;12:28. https://doi.org/10.4103/jpi.jpi_36_20.
29. Bai Y, Cole K, Martinez-Morilla S, Ahmed FS, Zugazagoitia J, Staaf J, et al. An open-source, automated tumor-infiltrating lymphocyte algorithm for prognosis in triple-negative breast cancer. Clin Cancer Res. 2021;27:5557–65. https://doi.org/10.1158/1078-0432.CCR-21-0325.
30. Hiltunen N, Väyrynen JP, Böhm J. Helminen OCD3$^+$, CD8$^+$, CD4$^+$ and FOXP3$^+$ T cells in the immune microenvironment of small bowel neuroendocrine tumors. Diseases. 2021;9:42. https://doi.org/10.3390/diseases9020042.
31. Hendry S, Salgado R, Gevaert T, Russell PA, John T, Thapa B, et al. Assessing tumor-infiltrating lymphocytes in solid tumors: a practical review for pathologists and proposal for a standardized method from the International Immunooncology Biomarkers Working Group: Part 1: assessing the host immune response, TILs in invasive breast carcinoma and ductal carcinoma in situ, metastatic tumor deposits and areas for further research. Adv Anat Pathol. 2017;24:235–51. https://doi.org/10.1097/PAP.0000000000000162.
32. Hirsch FR, McElhinny A, Stanforth D, Ranger-Moore J, Jansson M, Kulangara K, et al. PD-L1 immunohistochemistry assays for lung cancer: results from phase 1 of the blueprint PD-L1 IHC assay comparison project. J Thorac Oncol. 2017;12:208–22. https://doi.org/10.1016/j.jtho.2016.11.2228.
33. Huang J, Detterbeck FC, Wang Z, Loehrer PJ. Standard outcome measures for thymic malignancies. J Thorac Oncol. 2010;5:2017–23. https://doi.org/10.1097/JTO.0b013e3181f13682.
34. Teng MW, Ngiow SF, Ribas A, Smyth MJ. Classifying cancers based on T-cell Infiltration and PD-L1. Cancer Res. 2015;75:2139–45. https://doi.org/10.1158/0008-5472.CAN-15-0255.
35. Barua S, Fang P, Sharma A, Fujimoto J, Wistuba I, Rao AU, et al. Spatial interaction of tumor cells and regulatory T cells correlates with survival in non-small cell lung cancer. Lung Cancer. 2018;117:73–9. https://doi.org/10.1016/j.lungcan.2018.01.022.
36. Huang CY, Chiang SF, Ke TW, Chen TW, You YS, Chen WT, et al. Clinical significance of programmed death 1 ligand-1 (CD274/PD-L1) and intra-tumoral CD8+ T-cell infiltration in stage II-III colorectal cancer. Sci Rep. 2018;8:15658. https://doi.org/10.1038/s41598-018-33927-5.
37. Yokoyama S, Miyoshi H, Nishi T, Hashiguchi T, Mitsuoka M, Takamori S, et al. Clinicopathologic and prognostic implications of programmed death ligand 1 expression in thymoma. Ann Thorac Surg. 2016;101:1361–9. https://doi.org/10.1016/j.athoracsur.2015.10.044.
38. Spranger S, Spaapen RM, Zha Y, Williams J, Meng Y, Ha TT, et al. Up-regulation of PD-L1, IDO, and T(regs) in the melanoma tumor microenvironment is driven by CD8(+) T cells. Sci Transl Med. 2013;5:200ra116. https://doi.org/10.1126/scitranslmed.3006504.
39. Savas P, Salgado R, Denkert C, Sotiriou C, Darcy PK, Smyth MJ, et al. Clinical relevance of host immunity in breast cancer: from TILs to the clinic. Nat Rev Clin Oncol. 2016;13:228–41. https://doi.org/10.1038/nrclinonc.2015.215.
40. Shang B, Liu Y, Jiang SJ, Liu Y. Prognostic value of tumor-infiltrating FoxP3+ regulatory T cells in cancers: a systematic review and meta-analysis. Sci Rep. 2015;5:15179. https://doi.org/10.1038/srep15179.
41. Venet F, Pachot A, Debard AL, Bohe J, Bienvenu J, Lepape A, et al. Human CD4+CD25+ regulatory T lymphocytes inhibit lipopolysaccharide-induced monocyte survival through a Fas/Fas ligand-dependent mechanism. J Immunol. 2006;177:6540–7. https://doi.org/10.4049/jimmunol.177.9.6540.
42. Erdman SE, Sohn JJ, Rao VP, Nambiar PR, Ge Z, Fox JG, et al. CD4+CD25+ regulatory lymphocytes induce regression of intestinal tumors in ApcMin/+ mice. Cancer Res. 2005;65:3998–4004. https://doi.org/10.1158/0008-5472.CAN-04-3104.
43. Taube JM, Klein A, Brahmer JR, Xu H, Pan X, Kim JH, et al. Association of PD-1, PD-1 ligands, and other features of the tumor immune microenvironment with response to anti-PD-1 therapy. Clin Cancer Res. 2014;20:5064–74. https://doi.org/10.1158/1078-0432.CCR-13-3271.
44. Kalbasi A, Rengan R. Clinical experiences of combining immunotherapy and radiation therapy in non-small cell lung cancer: lessons from melanoma. Transl Lung Cancer Res. 2017;6:169–77. https://doi.org/10.21037/tlcr.2017.03.03.
45. Giaccone G, Kim C, Thompson J, McGuire C, Kallakury B, Chahine JJ, et al. Pembrolizumab in patients with thymic carcinoma: a single-arm, single-centre, phase 2 study. Lancet Oncol. 2018;19:347–55. https://doi.org/10.1016/S1470-2045(18)30062-7.
46. Cho J, Kim HS, Ku BM, Choi YL, Cristescu R, Han J, et al. Pembrolizumab for patients with refractory or relapsed thymic epithelial tumor: an open-label phase II trial. J Clin Oncol. 2019;37:2162–70. https://doi.org/10.1200/JCO.2017.77.3184.
47. Konstantina T, Konstantinos R, Anastasios K, Anastasia M, Eleni L, Ioannis S, et al. Fatal adverse events in two thymoma patients treated with anti-PD-1 immune check point inhibitor and literature review. Lung Cancer. 2019;135:29–32. https://doi.org/10.1016/j.lungcan.2019.06.015.
48. Yamamoto Y, Iwahori K, Funaki S, Matsumoto M, Hirata M, Yoshida T, et al. Immunotherapeutic potential of CD4 and CD8 single-positive T cells in thymic epithelial tumors. Sci Rep. 2020;10:4064. https://doi.org/10.1038/s41598-020-61053-8.
49. Giaccone G, Kim C. Durable response in patients with thymic carcinoma treated with pembrolizumab after prolonged follow-up. J Thorac Oncol. 2021;16:483–5. https://doi.org/10.1016/j.jtho.2020.11.003.
50. Rajan A. Immunotherapy for thymic cancers: a convoluted path toward a cherished goal. J Thorac Oncol. 2021;16:352–4. https://doi.org/10.1016/j.jtho.2020.12.007.
51. Thanner J, Bekos C, Veraar C, Janik S, Laggner M, Boehm PM, et al. Heat shock protein 90α in thymic epithelial tumors and non-thymomatous myasthenia gravis. Oncoimmunology. 2020;9:1756130. https://doi.org/10.1080/2162402X.2020.1756130.
52. Abu Hejleh T, Furqan M, Ballas Z, Clamon G. The clinical significance of soluble PD-1 and PD-L1 in lung cancer. Crit Rev Oncol Hematol. 2019;143:148–52. https://doi.org/10.1016/j.critrevonc.2019.08.009.
53. Sun P, Garrison LP. Retrospective outcomes studies for orphan diseases: challenges and opportunities. Curr Med Res Opin. 2012;28:665–7. https://doi.org/10.1185/03007995.2012.673480.

ACKNOWLEDGEMENTS

Thanks to Professor Federico Quaini (University Hospital of Parma, Department of Haematology and Bone Marrow Transplantation) for the scientific support. The authors wish to thank Andrea Alvarez-Hernandez for providing excellent immunohistochemistry technical assistance.

AUTHOR CONTRIBUTIONS

Concept and design: GB, A-IS, BM; development of methodology: GB, A-IS, LM, JT, JB, FT, ML; acquisition of data: JT, JB, FT, CV, analysis and interpretation of data: GB, JT, JB, ML, JRM, HJA, BM; writing, review and/or revision of the manuscript: GB, A-IS, LM, CV, WK, KH, JRM, HJA, BM; study supervision: WK, KH, HJA.

FUNDING

This work was supported by the research laboratories ARGE Moser and ARGE Ankersmit (APOSEC Project); FOLAB Chirurgie – Department of Surgery, Medical University Vienna.

COMPETING INTERESTS

The authors declare no competing interests.

ETHICS APPROVAL AND CONSENT TO PARTICIPATE

Written informed consent was provided by all patients. Tumour tissue specimens were collected by the Thoracic Surgery Unit of University Hospital of Vienna, Austria. The collection and study of these tissues were approved by the Institutional Ethics Committee of the Medical University of Vienna (EC#1053/2016) and conformed to the ethical guidelines of the Declaration of Helsinki.

ADDITIONAL INFORMATION

Supplementary information The online version contains supplementary material available at https://doi.org/10.1038/s41416-022-01875-7.

Correspondence and requests for materials should be addressed to Bernhard Moser.

Reprints and permission information is available at http://www.nature.com/reprints

Publisher's note Springer Nature remains neutral with regard to jurisdictional claims in published maps and institutional affiliations.